NIH Public Access
Author Manuscript
*J Chem Theory Comput*. Author manuscript; available in PMC 2012 January 11.

Published in final edited form as:
*J Chem Theory Comput*. 2011 January 11; 7(1): 1–3. doi:10.1021/ct100467t.

# Active participation of $Mg^{2+}$ ion in the reaction coordinate of RNA self-cleavage catalyzed by the hammerhead ribozyme

**Kin-Yiu Wong**[1], **Tai-Sung Lee**[2], and **Darrin M. York**[1,2]

Darrin M. York: york@biomaps.rutgers.edu

[1] Department of Chemistry, University of Minnesota, 207 Pleasant St. SE, Minneapolis, MN 55455, USA

[2] BioMaPS Institute and Department of Chemistry and Chemical Biology, Rutgers, The State University of New Jersey, 610 Taylor Rd., Piscataway, NJ 08854-8087, USA

Small self-cleaving ribozymes such as the hammerhead ribozyme (HHR) have been instrumental as model systems for RNA catalysis.[1–3] Recently, an extended HHR structure was determined by X-ray crystallography at 2.0-Å resolution,[4] in which a divalent metal ion was observed near the active site. Subsequent computer simulations lend credence to the possibility that this metal ion may play an active role in catalysis,[4,5] although free energy profiles to elucidate specific pathways have not yet been reported.

We report results from combined quantum mechanical/molecular mechanical (QM/MM) free energy simulations to explore metalassisted phosphoryl transfer and general acid catalysis in the extended HHR. The mechanisms considered here assumes that the 2′OH group of C17 has already been activated (i.e., is deprotonated) and acts as a nucleophile to go on an in-line attack to the adjacent scissile phosphate, passing through a pentavalent phosphorane intermediate/transition state, followed by acid-catalyzed departure of the O5′ leaving group of C1.1. The general acid is assumed to be the 2′OH group of G8.[6–8]

A series of six 2D potential of mean force (PMF) profiles are herein reported, requiring an aggregate of over 100 ns of QM/MM simulation. Simulations were based on the extended HHR solvent structure (PDB: 2OEU)[4] solvated by over 10K water molecules. Active site residues (G8, A9, C1.1, C17, and an $Mg^{2+}$ ion with coordinated water molecules shown in Figure 3) were treated quantum mechanically (81 atoms total) using the AM1/d-PhoT quantum model[9] with AM1/d model for $Mg^{2+}$.[10] We used the all-atom AMBER parmbsc0 force field,[11] to describe the HHR outside of the active site, along with the TIP4P-Ewald water model[12] and the consistent set of monovalent ion parameters.[13] Multidimensional PMF profiles were generated along reaction coordinates corresponding to phosphoryl transfer, proton transfer from the general acid to the leaving group, and divalent metal ion binding mode. Complete details are given in the Supporting Information.

## Phosphoryl transfer and general acid steps are stepwise, and sensitive to $Mg^{2+}$ binding mode

Our initial attempts to study the chemical steps of the HHR reaction from 2D PMF profiles using phosphoryl transfer and proton transfer reaction coordinates, but not considering a

Correspondence to: Darrin M. York, `york@biomaps.rutgers.edu`.

Supporting Information **Available:** Additional computational details. This material is available free of charge via the Internet at http://pubs.acs.org.

NIH-PA Author Manuscript
NIH-PA Author Manuscript
NIH-PA Author Manuscript

NIH-PA Author Manuscript

NIH-PA Author Manuscript

NIH-PA Author Manuscript

reaction coordinate associated with $Mg^{2+}$ ion binding mode, led to free energy barriers that were unexpectedly high (~37 kcal/mol) compared to an estimated barrier of ~20 kcal/mol derived from the experimental rate of one turnover per minute in HHR catalysis.[14] We extended the calculations so as to include a 3D-PMF profiles with a course-grained reaction coordinate associated with the $Mg^{2+}$ binding mode, and confirmed the sensitivity of the barriers to the $Mg^{2+}$ ion position along the reaction coordinate. A common feature of the reaction mechanism derived from the 3D profile was that the phosphoryl transfer and general acid steps were stepwise (e.g., Fig. 2a), allowing these steps to be decoupled. Both the phosphoryl transfer and general acid steps of the reaction were coupled with $Mg^{2+}$ binding mode, and hence separate 2D profiles were generated for each step with a reaction coordinate corresponding to the $Mg^{2+}$ binding mode as a second dimension. Table 1 summarizes key average geometrical parameters, and free energy values for stationary points along the reaction. The corresponding reaction rate constants are depicted in Fig. 1

## Phosphoryl transfer is rate limiting and facilitated by electrostatic stabilization by $Mg^{2+}$

The phosphoryl transfer step is rate controlling, having a free energy barrier of approximately 24.4 kcal/mol. The position of the $Mg^{2+}$ ion follows the negative charge along the phosphoryl transfer reaction coordinate in order to provide electrostatic stabilization. The change in the $Mg^{2+}$ position is continuous and monotonic throughout the phosphoryl transfer step (Fig. 2b), and is most pronounced in the initial and final stages when the nucleophile and leaving group have the greatest negative charge. The transition state is late (Fig. 3), having a P-O5′ distance of 2.11 Å. As the P-O5′ bond breaks, the $Mg^{2+}$ ion forms an inner-sphere coordination, leading to a $Mg^{2+}$-bound O5′ alkoxide intermediate.

## General acid catalysis is concerted with changes in $Mg^{2+}$ binding mode

The general acid step considered here assumes the 2′OH of G8 acts as a general acid catalyst to transfer a proton to the O5′ leaving group. Examination in Fig. 2c indicates that proton transfer occurs after formation of the $Mg^{2+}$-coordinated cleaved intermediate, and is concerted with changes in $Mg^{2+}$ binding mode. Unlike the phosphoryl transfer step, participation of the $Mg^{2+}$ along the reaction coordinate is most pronounced not at the endpoints of the step, but near the midpoint where the proton transfer occurs.

The free energy barrier for the transition state of the general acid step (Fig. 3) is 13.7 kcal/mol with respect to the activated precursor state. The intermediate is only 6.7 kcal/mol lower in free energy than the activated precursor, and has a 20.4 kcal/mol barrier to breakdown into the product state with a proton fully transferred to the O5′ leaving group.

## Relation with experiment

The present work explores a specific mechanistic scenario, departing from the activated precursor state, that assumes the catalytic metal ion is in a position bridging the A9 and scissile phosphates, and the 2′OH of G8 acts as a general acid catalyst. The former metal ion binding mode has not yet been observed experimentally, but has been inferred from biochemical experiments on the minimal[15] and extended[16] HHR, and predicted by molecular simulations.[5,17,18] The latter role of G8 is consistent from structural[4] and biochemical data.[6–8] There has been seminal work in the study of metal ion interactions for the minimal HHR.[19, 20] Time-resolved NMR experiments suggest that there is a dynamic equilibrium between energetically similar conformations in the minimal HHR that are sensitive to $Mg^{2+}$ binding,[21] and it has been suggested that the minimal and extended HHR may utilize a similar dynamic reaction mechanism for catalysis.[22] In the present study, we

NIH-PA Author Manuscript

NIH-PA Author Manuscript

NIH-PA Author Manuscript

provide computational support for the plausibility of a cleavage mechanism where phosphoryl transfer and general acid catalysis are stepwise, and that the catalytic divalent metal ion plays an active role in the chemical steps of catalysis. It is the hope that this work, together with experimental work that probes the nature of metal ion interactions at the active site, will provide deeper insight into the underpinnings of chemical catalysis in the HHR.

## Supplementary Material

Refer to Web version on PubMed Central for supplementary material.

## Acknowledgments

The authors are grateful for support from the National Institutes of Health (GM62248 to DY) and the Minnesota Supercomputing Institute (MSI). We thank Professor Victoria J. DeRose for useful comments on the manuscript.

## References

1. Strobel SA, Cochrane JC. Curr Opin Chem Biol 2007;11:636–643. [PubMed: 17981494]
2. Scott WG. Curr Opin Struct Biol 2007;17:280–286. [PubMed: 17572081]
3. Leclerc F. Molecules 2010;15:5389–5407. [PubMed: 20714304]
4. Martick M, Lee TS, York DM, Scott WG. Chem Biol 2008;15:332–342. [PubMed: 18420140]
5. Lee TS, Silva Lopez C, Giambaşu GM, Martick M, Scott WG, York DM. J Am Chem Soc 2008;130:3053–3064. [PubMed: 18271579]
6. Blount KF, Uhlenbeck OC. Annu Rev Biophys Biomol Struct 2005;34:415–440. [PubMed: 15869397]
7. Nelson JA, Uhlenbeck OC. RNA 2008;14:605–615. [PubMed: 18287565]
8. Thomas JM, Perrin DM. J Am Chem Soc 2009;131:1135–1143. [PubMed: 19154176]
9. Nam K, Cui Q, Gao J, York DM. J Chem Theory Comput 2007;3:486–504.
10. Imhof P, Noé F, Fischer S, Smith JC. J Chem Theory Comput 2006;2:1050–1056.
11. Pérez, Alberto; Marchán, Iván; Svozil, D.; Sponer, J.; C, TE., III; Laughton, CA.; Orozco, M. Biophys J 2007;92:3817–3829. [PubMed: 17351000]
12. Horn HW, Swope WC, Pitera JW, Madura JD, Dick TJ, Hura GL, Head-Gordon T. J Chem Phys 2004;120:9665–9678. [PubMed: 15267980]
13. Joung IS, Cheatham TE III. J Phys Chem B 2008;112:9020–9041. [PubMed: 18593145]
14. Scott, WG. What can the New Hammerhead Ribozyme Structures Teach us About Design?. In: Erdmann, V.; Barciszewski, J., editors. RNA Technologies and Their Applications. Springer-Verlag; 2010.
15. Wang S, Karbstein K, Peracchi A, Beigelman L, Herschlag D. Biochemistry 1999;38:14363–14378. [PubMed: 10572011]
16. Osborne EM, Schaak JE, Derose VJ. RNA 2005;11:187–196. [PubMed: 15659358]
17. Lee TS, Silva-Lopez C, Martick M, Scott WG, York DM. J Chem Theory Comput 2007;3:325–327. [PubMed: 19079784]
18. Lee TS, Giambaşu GM, Sosa CP, Martick M, Scott WG, York DM. J Mol Biol 2009;388:195–206. [PubMed: 19265710]
19. Vogt M, Lahiri S, Hoogstraten CG, Britt DR, DeRose VJ. J Am Chem Soc 2006;128:16764–16770. [PubMed: 17177426]
20. Osborne EM, Ward WL, Ruehle MZ, DeRose VJ. Biochemistry 2009;48:10654–10664. [PubMed: 19778032]
21. Fürtig B, Richter C, Schell P, Wenter P, Pitsch S, Schwalbe H. RNA Biol 2008;5:41–48. [PubMed: 18388486]
22. Nelson JA, Uhlenbeck OC. RNA 2008;14:43–54. [PubMed: 17998291]

**Figure 1.**
Schematic diagram for relative free-energy barriers and the corresponding reaction rate constants.

NIH-PA Author Manuscript
NIH-PA Author Manuscript
NIH-PA Author Manuscript

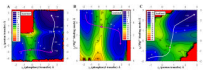

**Figure 2.**
(A) Selected 2D surface, harmonically restrained along the course-grained metal ion binding coordinate at $d(Mg^{2+},G8{:}O2')$ = 2.5Å, where $z_1 = d(O5',P) - d(P,O2')$, $z_2 = d(G8{:}O2',H) - d(H,O5')$. (B) 2D PMF for $Mg^{2+}$ binding mode in phosphoryl transfer step, where $z_4 = d(Mg^{2+},O5') + d(Mg^{2+},G8{:}O2')$. (C) 2D PMF for $Mg^{2+}$ binding mode in general acid step, where $z_5 = d(Mg^{2+},O5') - d(Mg^{2+},G8{:}O2')$. $d$(x,y) denotes distance between x and y. TS is the acronym of transition state.



NIH-PA Author Manuscript NIH-PA Author Manuscript NIH-PA Author Manuscript

NIH-PA Author Manuscript

NIH-PA Author Manuscript

NIH-PA Author Manuscript

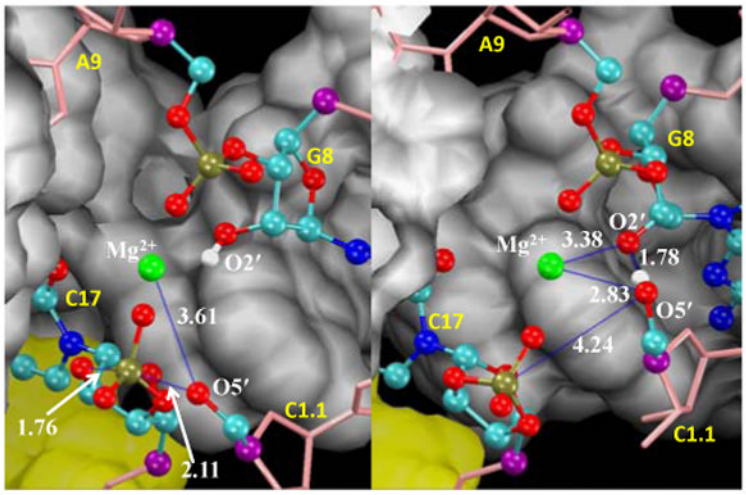


**Figure 3.**
Snapshots of the active site at the transition states for phosphoryl transfer (left) and general acid catalysis (right) with average distances labeled.

NIH-PA Author Manuscript NIH-PA Author Manuscript NIH-PA Author Manuscript



**Table 1**

Relative free energies and internuclear distances at various states of RNA self-cleavage catalysis in hammerhead ribozymes[a]

| | React. | $TS_1$ | Int. | $TS_2$ | Prod. |
|---|---|---|---|---|---|
| Nu-P | 3.50(04) | 1.76(05) | 1.66(03) | 1.67(03) | 1.68(03) |
| P-Lea | 1.65(03) | 2.11(05) | 4.51(04) | 4.24(48) | 3.63(23) |
| gA-H | 0.96(00) | 0.96(00) | 0.96(00) | 1.78(04) | 3.75(04) |
| H-Lea | 2.57(51) | 4.07(47) | 4.13(73) | 1.04(03) | 1.00(03) |
| $Mg^{2+}$-Lea | 3.99(18) | 3.61(17) | 2.02(05) | 2.83(86) | 4.48(05) |
| $Mg^{2+}$-gA | 4.56(18) | 4.03(18) | 4.33(06) | 3.38(86) | 2.03(05) |
| ΔG | 0.0(4) | 24.4(6) | -6.7(3) | 13.7(7) | -13.6(9) |

[a]Free energies (ΔG) are in kcal/mol, which were extracted from 1D PMF profiles along the minimum free-energy path through the 2D profiles. Average distances (X-Y) are in Å. Standard deviations are listed in parentheses divided by the decimal precision of the average values. The abbreviations “React”, “TS”, “Int”, and “Prod” signify reactant, transition, intermediate, and product states, respectively, and for the distance metrics, “Nu”, “Lea”, “gA” and “H” refer to the O2′ nucleophile, O5′ leaving group, general acid residues G8:O2′ and H2′, respectively.

*J Chem Theory Comput*. Author manuscript; available in PMC 2012 January 11.